Interacting moving bottlenecks in traffic flow

Paola Goatin, Chiara Daini, Maria Laura Delle Monache, Antonella Ferrara

Manuscript submitted to AIMS Journal

doi:10.3934/xx.xxxxxxx

INTERACTING MOVING BOTTLENECKS IN TRAFFIC FLOW

Paola Goatin*

Université Côte d'Azur, Inria, CNRS, LJAD
Sophia Antipolis, France

Chiara Daini

Inria Paris, Kopernic Research Group
Paris, France

Maria Laura Delle Monache

Department of Civil and Environmental Engineering
University of California, Berkeley
Berkeley, CA, 94720, USA

Antonella Ferrara

Department of Electrical, Computer and Biomedical Engineering
University of Pavia
Pavia, Italy

(Communicated by the associate editor name)

Abstract. We present a general multi-scale approach for modeling the interaction of controlled autonomous vehicles (AVs) with the surrounding traffic flow. The model consists of a scalar conservation law for the bulk traffic, coupled with ordinary differential equations describing the possibly interacting AV trajectories. The coupling is realized through flux constraints at the moving bottleneck positions, inducing the formation of non-classical jump discontinuities in the traffic density. In turn, AVs are forced to adapt their speed to the downstream traffic average velocity in congested situations.
We analyze the model solutions in a Riemann-type setting, and propose an adapted finite volume scheme to compute approximate solutions for general initial data.

The work paves the way to the study of general optimal control strategies for AV velocities, aiming at improving the overall traffic flow by reducing congestion phenomena and the associated externalities.

1. **Introduction.** Moving bottleneck models have been introduced in the engineering literature starting from the end of the last century to describe the interaction of slow moving vehicles, such as buses or trucks, with bulk traffic, see [9, 30, 28]. Further approaches have then be proposed in the applied mathematics community [1, 15, 27, 39, 41], always following the underlying idea of using multi-scale

2020 *Mathematics Subject Classification.* 90B20, 35L65.

Key words and phrases. Conservation laws; PDE-ODE systems; macroscopic traffic flow models; moving bottlenecks; autonomous vehicles.

The second author was partially supported by ERASMUS+/KA1 "NORTH SOUTH TRAINEESHIP" academic year 2020/21.

*Corresponding author: Paola Goatin.

models consisting of Partial Differential Equations (PDEs) to model the overall traffic flow evolution, coupled with Ordinary Differential Equations (ODEs) accounting for the moving bottlenecks trajectories. Despite the intrinsic difficulties arising as a result of the flux constraint induced by the presence of the slow vehicles, corresponding existence and stability results have been provided, see also [17, 20, 31, 32], together with numerical schemes to compute approximate solutions capturing the emerging non-classical phenomena [2, 3, 11, 14, 16].

More recently, moving bottleneck models have been applied to traffic flow regulation by means of Autonomous Vehicles (AVs), see e.g. [4, 5, 6, 7, 8, 34]. Indeed, AVs can act as endogenous actuators of moving variable speed limits, improving throughput by hindering upstream traffic. This possibility has already been the object of several theoretical studies (see e.g. [13, 24, 26, 35, 40, 42] and [19, Chapter 11]), but also artificial [25] and real world [38] experiments. In particular, it has been demonstrated that even low AV penetration rates can have a significant impact on reducing congestion phenomena and the associated energy consumption. In this context, macroscopic approaches are needed to address the curse of dimensionality in control design for microscopic models [18].

Even if some of the above works account for the presence of multiple AVs on the road, very few of them allow for AV interactions, and only in very specific modeling frameworks [21, 37]. In this paper, we aim at generalizing the control framework designed in [20, 34] for the Lighthill-Whitham-Richards model [33, 36] to multiple, possibly interacting, moving bottlenecks, as if they were distributed on several lanes and they were allowed both to merge (if on the same lane) and to overtake (if on different lanes). This can be achieved by a careful study of the corresponding Riemann-type problems, and a natural generalization of the numerical reconstruction technique presented in [3].
The proposed model can be used to develop a general simulation environment accounting for several AVs interacting with the surrounding traffic flow and among themselves, which in turns allows to design optimization-based control strategies having fleets of AVs as actuators.

The paper is organized as follows: Section 2 details the model framework, providing a mathematical description of the fully coupled PDE-ODE model and the interactions among AVs at the level of Riemann problems. Section 3 describes the numerical scheme and Section 4 shows the results of the numerical experiments.

2. PDE-ODE model with interacting moving bottlenecks.

Following [15, 20], we consider the following strongly coupled PDE-ODEs system

$$\partial_t \rho\,(t,x) + \partial_x f\,(\rho\,(t,x)) = 0,, \tag{1a}$$

$$\dot{y}_\ell(t) = \min\{u_\ell(t), v(\rho(t, y_\ell(t)+))\}, \tag{1b}$$

$$f\,(\rho\,(t,y_\ell(t))) - \dot{y}_\ell(t)\rho\,(t,y_\ell(t)) \le F_\alpha\,(\dot{y}_\ell(t)) := \max_{\rho\in[0,R]} \left(\alpha f(\rho/\alpha) - \rho\dot{y}_\ell(t)\right), \tag{1c}$$

$$\rho(0,x) = \rho_0(x), \tag{1d}$$

$$y_\ell(0) = y_\ell^0, \tag{1e}$$

for $\ell = 1,\dots,N$ and $t > 0$, $x \in \mathbb{R}$, where $\rho = \rho(t,x) \in [0,R]$ denotes the macroscopic traffic density at time $t \ge 0$ and at position $x \in \mathbb{R}$, $f = f(\rho) = \rho v(\rho)$ is the (strictly convex) flux and $v \in \mathbf{C^2}\,([0,R];[0,V])$ is a strictly decreasing function such that $v(0) = V$ and $v(R) = 0$, which represents the average speed of cars (R being

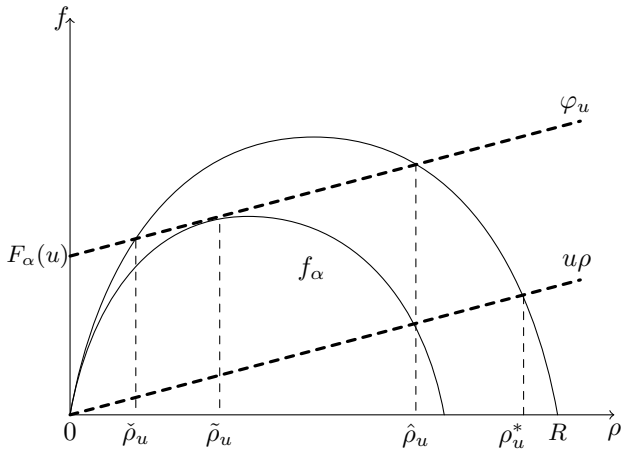

FIGURE 1. The definition of $\tilde\rho_u$, $\check\rho_u$, $\hat\rho_u$ and ρ_u^*.

the maximal vehicle density attainable on the considered road section). Above, $\rho_0 \in [0,R]$ and $y_\ell^0 \in \mathbb{R}$, $\ell = 1,\dots,N$, are respectively the initial traffic density and AV positions, while the function F_α in (1c), $\alpha \in]0,1[$, represents the road capacity reduction rate due to the presence of the AV at $x = y_\ell(t)$, $\ell = 1,\dots,N$, acting as a moving bottleneck which imposes a unilateral flux constraint at its position. For simplicity, we assume that this parameter is the same for all AVs, and it is a function of the number of lanes: $\alpha = (M-1)/M$, where $M \in \mathbb{N}$ denotes the number of lanes. (The extension to a more general framework would follow the same lines detailed in this work.) To determine the function F_α, we consider the rescaled flux function

$$\begin{array}{rccc} f_\alpha: & [0,\alpha R] & \longrightarrow & \mathbb{R}^+ \\ & \rho & \longmapsto & \rho v(\rho/\alpha) = \alpha f(\rho/\alpha), \end{array}$$

which is strictly concave function and such that $f_\alpha(0) = f_\alpha(\alpha R) = 0$. For every $u \in [0,V]$, we define the point $\tilde\rho_u$ as the unique solution to the equation $f_\alpha'(\rho) = u$. Moreover, for every $u \in [0,V]$, we define the function

$$\begin{array}{rccc} \varphi_u: & [0,R] & \longrightarrow & \mathbb{R}^+ \\ & \rho & \longmapsto & f_\alpha(\tilde\rho_u) + u\,(\rho - \tilde\rho_u)\,. \end{array}$$

Hence, if $\dot y(t) = u$, the function F_α in (1c) is defined by

$$\begin{array}{rccc} F_\alpha: & [0,V] & \longrightarrow & \mathbb{R}^+ \\ & u & \longmapsto & \varphi_u(0) = f_\alpha(\tilde\rho_u) - u\tilde\rho_u. \end{array}$$

If $\dot y(t) = v(\rho(t,y(t)+))$, the inequality (1c) is trivially satisfied since the left-hand side is zero. Finally, the points $0 \le \check\rho_u \le \tilde\rho_u \le \hat\rho_u \le \rho_u^* \le R$ are uniquely defined by

$$\check\rho_u = \min \mathcal{I}_u, \quad \hat\rho_u = \max \mathcal{I}_u, \quad \mathcal{I}_u = \{\rho \in [0,R] :\, f(\rho) = \varphi_u(\rho)\}\,, \quad v(\rho_u^*) = u,$$

see [15, 20] and Figure 1. We remark that $\check\rho_V = \tilde\rho_V = \hat\rho_V = \rho_V^* = 0$.

Solutions to (1) are defined as follows (see [20, Definition 3.1]):

Definition 2.1. The $N+1$-tuple $(\rho, y_1, \dots, y_N)$ provides a solution to (1) if the following conditions hold.

1. $\rho \in \mathbf{C^0}\left(\mathbb{R}^+; \mathbf{L^1_{loc}}\left(\mathbb{R}; [0,R]\right)\right)$ and $\mathrm{TV}\left(\rho(t)\right) < +\infty$ for all $t \in \mathbb{R}^+$;
2. $y_\ell \in \mathbf{W^{1,1}_{loc}}(\mathbb{R}^+; \mathbb{R})$ for $\ell = 1,\dots,N$;

3. For every $\kappa \in \mathbb{R}$ and for all $\varphi \in \mathbf{C_c^1}(\mathbb{R}^2;\mathbb{R}^+)$ it holds

$$\int_{\mathbb{R}^+}\int_{\mathbb{R}} (|\rho-\kappa|\partial_t\varphi + \mathrm{sgn}(\rho-\kappa)(f(\rho)-f(\kappa))\partial_x\varphi)\,dx\,dt + \int_{\mathbb{R}} |\rho_0-\kappa|\varphi(0,x)\,dx$$
$$+2\sum_{\ell=1}^{N}\int_{\mathbb{R}^+} \left(f(\kappa)-\dot y_\ell(t)\kappa - \min\{f(\kappa)-\dot y_\ell(t)\kappa, F_\alpha(\dot y_\ell(t))\}\right)\varphi(t,y(t))\,dt \geq 0\,;$$

4. For a.e. $t>0$, $f\left(\rho\left(t,y_\ell(t)\pm\right)\right) - \dot y_\ell(t)\rho\left(t,y_\ell(t)\pm\right) \leq F_\alpha\left(\dot y_\ell(t)\right)$ for $\ell = 1,\dots,N$;
5. For a.e. $t>0$, $\dot y_\ell(t) = \min\left\{u_\ell(t), v\left(\rho\left(t,y_\ell(t)+\right)\right)\right\}$ for $\ell = 1,\dots,N$.

As long as AV trajectories do not intersect, one can apply the theory and the numerical schemes developed in [3, 14, 15, 16, 20]. In particular, we recall that the Constrained Riemann Solver is defined as follows.

Definition 2.2. The Constrained Riemann Solver $\mathcal{R}^\alpha$ for

$$\partial_t\rho\left(t,x\right) + \partial_x f\left(\rho\left(t,x\right)\right) = 0, \tag{2a}$$
$$\dot y(t) = \min\{u, v(\rho(t,y(t)+))\}, \tag{2b}$$
$$f\left(\rho\left(t,y(t)\right)\right) - \dot y(t)\rho\left(t,y(t)\right) \leq F_\alpha\left(\dot y(t)\right), \tag{2c}$$
$$\rho(0,x) = \begin{cases}\rho_L & \text{if } x<0,\\ \rho_R & \text{if } x>0,\end{cases} \tag{2d}$$
$$y(0) = 0, \tag{2e}$$

is the map $\mathcal{R}^\alpha : [0,R]^2\times[0,V] \to \mathbf{L^1_{loc}}(\mathbb{R},[0,R])$ defined as follows.

1. If $f(\mathcal{R}(\rho_L,\rho_R)(u)) > F_\alpha(u) + u\,\mathcal{R}(\rho_L,\rho_R)(u)$, then
$$\mathcal{R}^\alpha(\rho_L,\rho_R;u)(x/t) = \begin{cases}\mathcal{R}(\rho_L,\hat\rho_u)(x/t) & \text{if } x<u\,t,\\ \mathcal{R}(\check\rho_u,\rho_R)(x/t) & \text{if } x\geq u\,t,\end{cases} \quad \text{and} \quad y(t) = u\,t.$$
2. If $f(\mathcal{R}(\rho_L,\rho_R)(u)) \leq F_\alpha(u) + u\,\mathcal{R}(\rho_L,\rho_R)(u)$, then
$$\mathcal{R}^\alpha(\rho_L,\rho_R;u) = \mathcal{R}(\rho_L,\rho_R) \quad \text{and} \quad y(t) = \min\{u, v(\rho_R)\}\,t.$$

Above, $\mathcal{R}$ denotes the standard (i.e. without the constraint (2c)) Riemann solver for (2a)-(2d), i.e. the (right continuous) map $(t,x)\mapsto \mathcal{R}(\rho_L,\rho_R)(x/t)$ given by the standard weak entropy solution to (2a)-(2d).

In this paper, we are interested in describing what happens when two vehicles AV_i and AV_j, with $i,j\in\{1,\dots,N\}$, $i\neq j$, interact. Let us assume $y_i(t) < y_j(t)$ with constant speeds $u_i(t) = u_i > u_j(t) = u_j$ for $t\in\,]\bar t-,_\varepsilon \bar t[$, so that $y_i(\bar t) = y_j(\bar t)$ for some $\bar t>0$, see Figure 2. Depending on the surrounding traffic density conditions, only three situations may occur in a Riemann-like setting (piece-wise constant density with at most one jump discontinuity):

- The constraint (1c) is enforced for $\ell = i$ (we will say that AV_i is *active*), so that $\rho(t,x) = \hat\rho_{u_i}$ for $x < y_i(t)$ and $\rho(t,x) = \check\rho_{u_i}$ for $x > y_i(t)$. Since, at $x = y_j(t)$, it holds $f\left(\check\rho_{u_i}\right) - u_j\check\rho_{u_i} \leq F_\alpha\left(u_j\right)$ (see Figure 2), the constraint is not enforced for $\ell = j$ (AV_j is then *inactive*).
- If AV_j is active, we have $\rho(t,x) = \hat\rho_{u_j}$ for $x < y_j(t)$ and $\rho(t,x) = \check\rho_{u_j}$ for $x > y_j(t)$. At $x = y_i(t)$, it therefore holds $f\left(\hat\rho_{u_j}\right) - u_i\hat\rho_{u_j} \leq F_\alpha\left(u_i\right)$, thus AV_i is *inactive*.

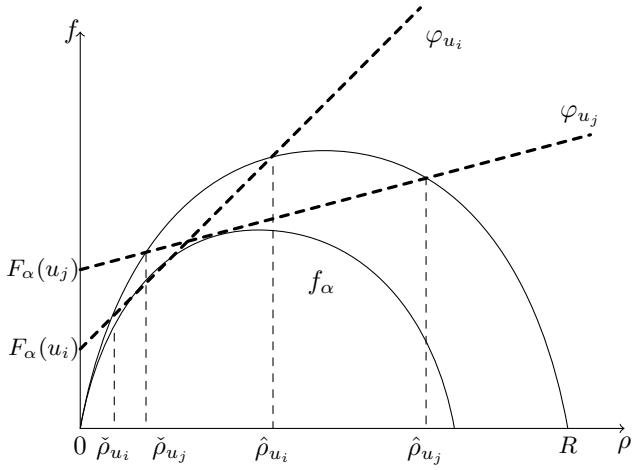

FIGURE 2. Notation for interacting bottlenecks.

- If both AV_i and AV_j are inactive, we may have either a constant density or a classical shock coinciding with one of the AV trajectories. In any case, the density must satisfy $\rho(t,x) \in [0, \check{\rho}_{u_i}] \cup [\hat{\rho}_{u_j}, R]$.

We remark that AV_i and AV_j cannot be both active at the same time, unless other waves are present between them.

To detail the problem evolution after the interaction (at $t > \bar{t}$), we distinguish if AVs are moving in different lanes or if they are located on the same lane.

Same lane interactions. Let us assume that the two vehicles are in the same lane, so for $t > \bar{t}$ the upstream vehicle must adapt to the downstream vehicle speed: we will have $y_i(t) = y_j(t)$ with $u_i(t) = u_j(t)$ for $t \geq \bar{t}$. Three situations may occur, see Figure 3:

- If, before the interaction, AV_i was active and AV_j inactive, at $t > \bar{t}$ the solution will consists of a classical shock joining $\hat{\rho}_{u_i}$ to $\hat{\rho}_{u_j}$, followed by a non-classical shock at $x = y_j(t) = y_i(t)$ between $\hat{\rho}_{u_j}$ and $\check{\rho}_{u_j}$ and a rarefaction wave from $\check{\rho}_{u_j}$ to $\check{\rho}_{u_i}$, see Figure 3a. In particular, after the interaction, both AVs will be active.
- If, before the interaction, AV_i was inactive and AV_j active, at $t > \bar{t}$ the solution will consists only of a non-classical shock joining $\hat{\rho}_{u_j}$ to $\check{\rho}_{u_j}$, see Figure 3b. Again, after the interaction, both AVs will be active.
- If, before the interaction, AV_i and AV_j were both inactive, at $t > \bar{t}$ the solution will consists at most of the classical shock that was already present before the interaction, see Figure 3c. After the interaction, both AVs will still be inactive.

In any case, after the interaction, the two vehicles behave as AV_j.

Different lane interactions. If the two interacting vehicles travel in different lanes, for $t > \bar{t}$ they will follow their own trajectory and AV_i will overtake AV_j: we will have $y_i(t) \geq y_j(t)$ with $u_i(t) \geq u_j(t)$ for $t \geq \bar{t}$. Three situations may occur, see Figure 4:

- If, before the interaction, AV_i was active and AV_j inactive, at $t > \bar{t}$ the solution will consists of a classical shock joining $\hat{\rho}_{u_i}$ to $\hat{\rho}_{u_j}$, followed by a non-classical shock at $x = y_j(t)$ from $\hat{\rho}_{u_j}$ to $\check{\rho}_{u_j}$, a classical shock from $\check{\rho}_{u_j}$ to $\hat{\rho}_{u_i}$ and a

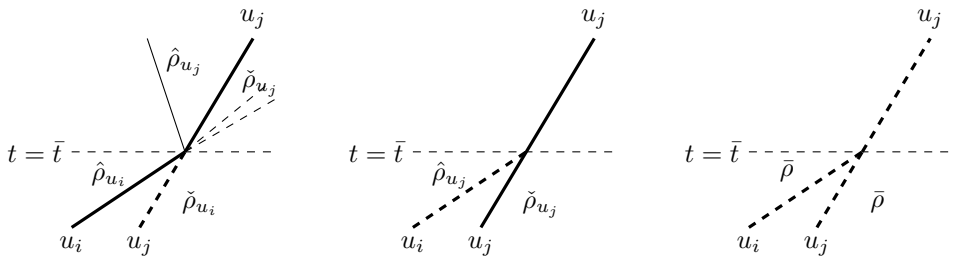

(A) AV_i active, AV_j not (B) AV_j active, AV_i not (C) AV_i, AV_j not active

FIGURE 3. Possible configurations of AV interactions on the same lane.

non-classical shock at $x = y_i(t)$ from $\hat{\rho}_{u_i}$ to $\check{\rho}_{u_i}$, see Figure 4a. In particular, after the interaction, both AVs will be active.

- If, before the interaction, AV_i was inactive and AV_j active, at $t > \bar{t}$ the solution will consists of a non-classical shock at $x = y_j(t)$ from $\hat{\rho}_{u_j}$ to $\check{\rho}_{u_j}$, followed by a classical shock from $\check{\rho}_{u_j}$ to $\hat{\rho}_{u_i}$, a non-classical shock at $x = y_i(t)$ from $\hat{\rho}_{u_i}$ to $\check{\rho}_{u_i}$ and a classical shock from $\check{\rho}_{u_i}$ to $\check{\rho}_{u_j}$, see Figure 4b. In particular, after the interaction, both AVs will be active.
- If, before the interaction, AV_i and AV_j were both inactive, at $t > \bar{t}$ the solution will consists at most of the classical shock that was already present before the interaction, see Figure 4c. After the interaction, both AVs will still be inactive.

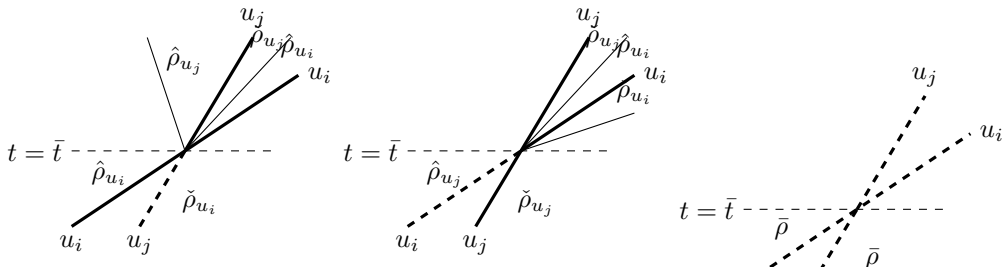

(A) $t < \bar{t}$: AV_i active, AV_j not
$t > \bar{t}$: both active

(B) $t < \bar{t}$: AV_j active, AV_i not
$t > \bar{t}$: both active

(C) AV_i, AV_j not active

FIGURE 4. Possible configurations of AV interactions on different lanes.

3. **Numerical scheme.** We extend the reconstruction strategy introduced in [3] to include moving bottleneck interactions. The scheme is composed of two parts:

Numerical approximation of (1a)-(1c). To approximate the conservation equation (1a), we use a conservative finite volume scheme for the constrained hyperbolic PDE using a flux reconstruction technique at the constraint locations, which allows to capture the non-classical shocks sharply. Let Δx and Δt be the fixed space and time steps satisfying the standard Courant-Friedrichs-Lewy (CFL) condition [10]:

$$\max_{\rho \in [0,R]} |f'(\rho)| \Delta t < \Delta x,$$

and set $x_{j-1/2} = j\Delta x$, $x_j = (j+1/2)\Delta x$ for $j \in \mathbb{Z}$, and $t^n = n\Delta t$ for $n \in \mathbb{N}$. The initial data ρ_0 is approximated by the piece-wise constant function obtained by averaging it on the discretization cells $C_j = [x_{j-1/2}, x_{j+1/2}[$, namely

$$\rho_j^0 = \frac{1}{\Delta x}\int_{x_{j-1/2}}^{x_{j+1/2}} \rho_0(x)\,dx, \qquad j \in \mathbb{Z}.$$

Away from AV positions, equation (1a) is approximated by the standard Godunov scheme [22], whose numerical fluxes at cell interfaces $F^n_{j+\frac{1}{2}} = F(\rho^n_j, \rho^n_{j+1})$ can in this case be derived using the supply-demand formula [29]

$$F(\rho^n_j, \rho^n_{j+1}) = \min\{D(\rho^n_j), S(\rho^n_{j+1})\}, \tag{3}$$

where

$$D(\rho) = f(\min\{\rho, \rho_{cr}\}), \quad S(\rho) = f(\max\{\rho, \rho_{cr}\}),$$

$\rho_{cr} = \operatorname{argmin}_{\rho\in[0,R]} f(\rho)$ being the point of maximum of the flux function f.
Let now the approximate ℓ-th AV position be $y^n_\ell \in C_{m_\ell}$ for some $m_\ell \in \mathbb{Z}$, $\ell = 1, \dots, N$. If

$$f(\mathcal{R}(\rho^n_{m_\ell-1}, \rho^n_{m_\ell+1})(u^n_\ell)) > F_\alpha(u^n_\ell) + u^n_\ell \mathcal{R}(\rho^n_{m_\ell-1}, \rho^n_{m_\ell+1})(u^n_\ell),$$

we assume a moving bottleneck at $\bar{x}_{m_\ell} = x_{m_\ell-1/2} + d^n_{m_\ell}\Delta x$ with $d^n_{m_\ell} = \dfrac{\check{\rho}_{u^n_\ell} - \rho^n_{m_\ell}}{\check{\rho}_{u^n_\ell} - \hat{\rho}_{u^n_\ell}}$.
If $0 \le d^n_{m_\ell} \le 1$, then $\bar{x}_{m_\ell} \in C_{m_\ell}$ and we set

$$\Delta t^n_{m_\ell} = \frac{1 - d^n_{m_\ell}}{u^n_\ell}\Delta x,$$

$$F^n_{m_\ell-\frac{1}{2}} = F(\rho^n_{m_\ell-1}, \hat{\rho}_{u^n_\ell}),$$

$$\Delta t F^n_{m_\ell+\frac{1}{2}} = \min\left(\Delta t^n_{m_\ell}, \Delta t\right) f(\check{\rho}_{u^n_\ell}) + \max\left(\Delta t - \Delta t^n_{m_\ell}, 0\right) f(\hat{\rho}_{u^n_\ell}).$$

We can then update the density by means of the conservative formula

$$\rho^{n+1}_j = \rho^n_j - \frac{\Delta t}{\Delta x}\left(F^n_{j+\frac{1}{2}} - F^n_{j-\frac{1}{2}}\right), \qquad j \in \mathbb{Z}. \tag{4}$$

Above, we set $u^n_\ell = u_\ell(t^n)$. If two or more AVs are located in the same cell, the moving bottlenecks are treated sequentially one after the other, starting from those which are not active (i.e. satisfy (1c)), then processing those which are active (violating (1c)).

Remark 1. For better resolution, we also apply the above reconstruction technique to classical shocks, as described in [3, Section 3.1].

Numerical approximation of (1b). To track the AV trajectories, at each time step, we update the positions y^n_ℓ using an explicit Euler scheme

$$y^{n+1}_\ell = y^n_\ell + v(\rho^n)\Delta t^n, \qquad \ell = 1, \dots, N.$$

If two AVs are in the same lane and in the same cell, and the upstream AV_{ℓ_1} moves faster than the downstream AV_{ℓ_2}, i.e. $u^n_{\ell_1} > u^n_{\ell_2}$, then we set

$$y^{n+1}_{\ell_1} = y^{n+1}_{\ell_2} = y^n_{\ell_2} + v(\rho^n)\Delta t^n \quad \text{and} \quad u^n_{\ell_1} = u^n_{\ell_2}.$$

(A more accurate computation of the interaction point could be implemented to improve simulation accuracy.)

Remark 2. The above procedure seems not coherent with the observation that two vehicles travelling at close speeds $u_i \approx u_j$ would act as a single bottleneck with $\alpha_{ij} = \alpha_i + \alpha_j - 1$. In this perspective, another option could be to reconstruct a single front moving at speed $u_{ij} = (u_i + u_j)/2$ with $\alpha = \alpha_{ij}$ whenever two vehicles are in the same cell on two different lanes. In this case, the procedure should be the following:

If $f(\mathcal{R}(\rho^n_{m-1}, \rho^n_{m+1})(u_{ij})) > F_{\alpha_{ij}}(u_{ij}) + u_{ij}\mathcal{R}(\rho^n_{m-1}, \rho^n_{m+1})(u_{ij})$,
we replace ρ^n_m by $\hat{\rho}_{u_{ij}}$ and $\check{\rho}_{u_{ij}}$, with the jump located at

$$\bar{x}_m = x_{m-\frac{1}{2}} + d^n_m \Delta x,$$

where $d^n_m \in [0, 1]$ is given by

$$d^n_m = \frac{\check{\rho}_{u_{ij}} - \rho_m}{\check{\rho}_{u_{ij}} - \hat{\rho}_{u_{ij}}}.$$

To reconstruct the numerical flux at the cell interface $x_{m+\frac{1}{2}}$, we compute

$$\Delta t_{m+\frac{1}{2}} = \frac{1 - d^n_m}{u_{ij}} \Delta x$$

and we set

$$\Delta t F^n_{m+\frac{1}{2}} = \min\{\Delta t_{m+\frac{1}{2}}, \Delta t\} f(\check{\rho}_{u_{ij}}) + \max\{\Delta t - \Delta t_{m+\frac{1}{2}}, 0\} f(\hat{\rho}_{u_{ij}}).$$

4. **Numerical tests.** In this section we illustrate the performances of the numerical scheme described in the previous Section 3 in capturing AV interactions correctly. We first analyze the Riemann-like cases described in Section 2, to conclude with a more general test case.

We consider a three lane stretch of road of length 50 km, parametrized by the interval $[0, 50]$ with absorbing boundary conditions. We consider the quadratic flux function proposed by Greenshields [23] that assumes a linear decreasing dependence of the speed on the traffic density

$$f(\rho) = V\rho\left(1 - \frac{\rho}{R}\right), \tag{5}$$

where $V = 140$ km/h denotes the maximal speed and $R = 400$ veh/km the maximal (bump-to-bump) density on the road. The capacity reduction ratio is set to $\alpha = 0.6$. In all simulations, we set $\Delta x = 0.2$ and $\Delta t = 0.9\Delta x/V$.

For the Riemann-like cases, we consider the following initial data:

$$AV_1 : \begin{cases} y_1(0) = 7.5, \\ u_1 = 50, \end{cases} \qquad AV_2 : \begin{cases} y_2(0) = 15, \\ u_2 = 20, \end{cases}$$

$$\text{(a) } \rho_0(x) = \begin{cases} \hat{\rho}_{u_1} \approx 210 & \text{if } x < 7.5, \\ \check{\rho}_{u_1} \approx 47 & \text{if } x > 7.5, \end{cases} \quad \text{(b) } \rho_0(x) = \begin{cases} \hat{\rho}_{u_2} \approx 280 & \text{if } x < 15, \\ \check{\rho}_{u_2} \approx 63 & \text{if } x > 15, \end{cases}$$

$$\text{(c) } \rho_0(x) \equiv 20.$$

The results are depicted in Figures 5 and 6. Except small spurious oscillations emerging from AV interactions in some cases, the solutions, and in particular non-classical shocks, are accurately reproduced.

To give a more general example, we consider the following initial data: $\rho_0(x) \equiv 200$ and

$$AV_1 : \begin{cases} y_1(0) = 2.5, \\ u_1 = 120, \end{cases} \qquad AV_2 : \begin{cases} y_2(0) = 7.5, \\ u_2 = 30, \end{cases}$$
$$AV_3 : \begin{cases} y_3(0) = 10, \\ u_3 = 55, \end{cases} \qquad AV_4 : \begin{cases} y_4(0) = 20, \\ u_4 = 20, \end{cases} \tag{6}$$

Moreover, AV_1 and AV_3 are on the same lane.
Figure 7 displays the solution, accounting for the different interaction types (queuing and overtaking). We observe that AV_1 and AV_3 are initially inactive while AV_2 and AV_4 are active. Moreover, AV_1 and AV_3 overtake the preceding vehicles and finally merge. Also, AV_1 is always inactive until it merges with AV_3, which becomes active after the interaction with AV_4, while AV_4 is always active. On the contrary, AV_2 becomes inactive when it reaches an high traffic density region.

5. **Conclusion.** We have presented a strongly coupled PDE-ODE model describing the interaction of a small number of autonomous vehicles with bulk traffic on a multi-lane highway. The model allows for AV queuing and overtaking, expanding the range of traffic control applications of previous works [4, 5, 6, 7, 8, 34]. A first study on traffic management opportunities offered by this framework is presented in [12], showing that low penetration rates are sufficient to reach nearly optimal improvements of a selected performance index.

REFERENCES

[1] R. Borsche, R. M. Colombo, and M. Garavello. Mixed systems: ODEs - balance laws. *J. Differential Equations*, 252(3):2311–2338, 2012.

[2] G. Bretti, E. Cristiani, C. Lattanzio, A. Maurizi, and B. Piccoli. Two algorithms for a fully coupled and consistently macroscopic PDE-ODE system modeling a moving bottleneck on a road. *Math. Eng.*, 1(1):55–83, 2019.

[3] C. Chalons, M. L. Delle Monache, and P. Goatin. A conservative scheme for non-classical solutions to a strongly coupled PDE-ODE problem. *Interfaces Free Bound.*, 19(4):553–570, 2017.

[4] M. Cičić, L. Jin, and K. H. Johansson. Coordinating vehicle platoons for highway bottleneck decongestion and throughput improvement, 2020.

[5] M. Cičić and K. H. Johansson. Traffic regulation via individually controlled automated vehicles: a cell transmission model approach. In *2018 21st International Conference on Intelligent Transportation Systems (ITSC)*, pages 766–771, 2018.

[6] M. Cičić and K. H. Johansson. Energy-optimal platoon catch-up in moving bottleneck framework. In *2019 18th European Control Conference (ECC)*, pages 3674–3679, 2019.

[7] M. Cičić and K. H. Johansson. Stop-and-go wave dissipation using accumulated controlled moving bottlenecks in multi-class CTM framework. In *2019 IEEE 58th Conference on Decision and Control (CDC)*, pages 3146–3151, 2019.

[8] M. Cičić, I. Mikolášek, and K. H. Johansson. Front tracking transition system model with controlled moving bottlenecks and probabilistic traffic breakdowns. *IFAC-PapersOnLine*, 53(2):14990–14996, 2020. 21st IFAC World Congress.

[9] C. G. Claudel and A. M. Bayen. Lax–Hopf Based Incorporation of Internal Boundary Conditions Into Hamilton-Jacobi Equation. Part II: Computational Methods. *IEEE Transactions on Automatic Control*, 55(5):1158–1174, 2010.

[10] R. Courant, K. Friedrichs, and H. Lewy. On the partial difference equations of mathematical physics. *IBM J. Res. Develop.*, 11:215–234, 1967.

[11] C. F. Daganzo and J. A. Laval. On the numerical treatment of moving bottlenecks. *Transportation Research Part B: Methodological*, 39(1):31–46, 2005.

[12] C. Daini, P. Goatin, M. L. Delle Monache, and A. Ferrara. Centralized Traffic Control via Small Fleets of Connected and Automated Vehicles. In *ECC 2022 - European Control Conference*, London, United Kingdom, July 2022.

[13] L. Davis. Effect of adaptive cruise control systems on traffic flow. *Physical Review E*, 69(6):066110, 2004.

[14] M. L. Delle Monache and P. Goatin. A front tracking method for a strongly coupled PDE-ODE system with moving density constraints in traffic flow. *Discrete Contin. Dyn. Syst. Ser. S*, 7(3):435–447, 2014.

[15] M. L. Delle Monache and P. Goatin. Scalar conservation laws with moving constraints arising in traffic flow modeling: an existence result. *J. Differential Equations*, 257(11):4015–4029, 2014.

[16] M. L. Delle Monache and P. Goatin. A numerical scheme for moving bottlenecks in traffic flow. *Bull. Braz. Math. Soc. (N.S.)*, 47(2):605–617, 2016. Joint work with C. Chalons.

[17] M. L. Delle Monache and P. Goatin. Stability estimates for scalar conservation laws with moving flux constraints. *Netw. Heterog. Media*, 12(2):245–258, 2017.

[18] M. L. Delle Monache, T. Liard, A. Rat, R. Stern, R. Bhadani, B. Seibold, J. Sprinkle, D. B. Work, and B. Piccoli. *Feedback Control Algorithms for the Dissipation of Traffic Waves with Autonomous Vehicles*, pages 275–299. Springer International Publishing, Cham, 2019.

[19] A. Ferrara, S. Sacone, and S. Siri. *Freeway traffic modelling and control*. Advances in Industrial Control. Springer, Cham, 2018.

[20] M. Garavello, P. Goatin, T. Liard, and B. Piccoli. A multiscale model for traffic regulation via autonomous vehicles. *J. Differential Equations*, 269(7):6088–6124, 2020.

[21] I. Gasser, C. Lattanzio, and A. Maurizi. Vehicular traffic flow dynamics on a bus route. *Multiscale Model. Simul.*, 11(3):925–942, 2013.

[22] S. K. Godunov. A difference method for numerical calculation of discontinuous solutions of the equations of hydrodynamics. *Mat. Sb. (N.S.)*, 47 (89):271–306, 1959.

[23] B. Greenshields, J. Bibbins, W. Channing, and H. Miller. A study of traffic capacity. In *Highway research board proceedings*, volume 1935. National Research Council (USA), Highway Research Board, 1935.

[24] M. Guériau, R. Billot, N.-E. El Faouzi, J. Monteil, F. Armetta, and S. Hassas. How to assess the benefits of connected vehicles? a simulation framework for the design of cooperative traffic management strategies. *Transportation Research Part C: Emerging Technologies*, 67:266–279, 2016.

[25] K. Jang, E. Vinitsky, B. Chalaki, B. Remer, L. Beaver, A. A. Malikopoulos, and A. Bayen. Simulation to scaled city: Zero-shot policy transfer for traffic control via autonomous vehicles. In *Proceedings of the 10th ACM/IEEE International Conference on Cyber-Physical Systems*, ICCPS '19, pages 291–300, New York, NY, USA, 2019. ACM.

[26] F. Knorr, D. Baselt, M. Schreckenberg, and M. Mauve. Reducing traffic jams via VANETs. *IEEE Transactions on Vehicular Technology*, 61(8):3490–3498, 2012.

[27] C. Lattanzio, A. Maurizi, and B. Piccoli. Moving bottlenecks in car traffic flow: a PDE-ODE coupled model. *SIAM J. Math. Anal.*, 43(1):50–67, 2011.

[28] J. Lebacque, J. Lesort, and F. Giorgi. Introducing buses into first-order macroscopic traffic flow models. *Transportation Research Record*, 1644(1):70–79, 1998.

[29] J.-P. Lebacque. The Godunov scheme and what it means for first order traffic flow models. In *Transportation and traffic theory. Proceedings of the 13th international symposium on transportation and traffic theory, Lyon, France, 24-26 JULY 1996*, 1996.

[30] L. Leclercq, S. Chanut, and J.-B. Lesort. Moving bottlenecks in Lighthill-Whitham-Richards model: A unified theory. *Transportation Research Record*, 1883(1):3–13, 2004.

[31] T. Liard and B. Piccoli. Well-posedness for scalar conservation laws with moving flux constraints. *SIAM J. Appl. Math.*, 79(2):641–667, 2019.

[32] T. Liard and B. Piccoli. On entropic solutions to conservation laws coupled with moving bottlenecks. *Commun. Math. Sci.*, 19(4):919–945, 2021.

[33] M. J. Lighthill and G. B. Whitham. On kinematic waves. II. A theory of traffic flow on long crowded roads. *Proc. Roy. Soc. London. Ser. A.*, 229:317–345, 1955.

[34] G. Piacentini, P. Goatin, and A. Ferrara. Traffic control via moving bottleneck of coordinated vehicles. *IFAC-PapersOnLine*, 51(9):13–18, 2018.

[35] G. Piacentini, M. Čičić, A. Ferrara, and K. Johansson. VACS equipped vehicles for congestion dissipation in multi-class ctm framework. In *2019 18th European Control Conference (ECC)*, pages 2203–2208, 2019.

[36] P. I. Richards. Shock waves on the highway. *Operations Res.*, 4:42–51, 1956.

[37] M. D. Simoni and C. G. Claudel. A fast simulation algorithm for multiple moving bottlenecks and applications in urban freight traffic management. *Transportation Research Part B: Methodological*, 104:238–255, 2017.

[38] R. E. Stern, S. Cui, M. L. D. Monache, R. Bhadani, M. Bunting, M. Churchill, N. Hamilton, R. Haulcy, H. Pohlmann, F. Wu, B. Piccoli, B. Seibold, J. Sprinkle, and D. B. Work. Dissipation of stop-and-go waves via control of autonomous vehicles: Field experiments. *Transportation Research Part C: Emerging Technologies*, 89:205 – 221, 2018.

[39] A. Sylla. Influence of a slow moving vehicle on traffic: well-posedness and approximation for a mildly nonlocal model. *Netw. Heterog. Media*, 16(2):221–256, 2021.

[40] A. Talebpour and H. S. Mahmassani. Influence of connected and autonomous vehicles on traffic flow stability and throughput. *Transportation Research Part C: Emerging Technologies*, 71:143–163, 2016.

[41] S. Villa, P. Goatin, and C. Chalons. Moving bottlenecks for the Aw-Rascle-Zhang traffic flow model. *Discrete Contin. Dyn. Syst. Ser. B*, 22(10):3921–3952, 2017.

[42] M. Wang, W. Daamen, S. P. Hoogendoorn, and B. van Arem. Cooperative car-following control: Distributed algorithm and impact on moving jam features. *IEEE Transactions on Intelligent Transportation Systems*, 17(5):1459–1471, 2016.

E-mail address: paola.goatin@inria.fr
E-mail address: chiara.daini@inria.fr
E-mail address: mldellemonache@berkeley.edu
E-mail address: antonella.ferrara@unipv.it

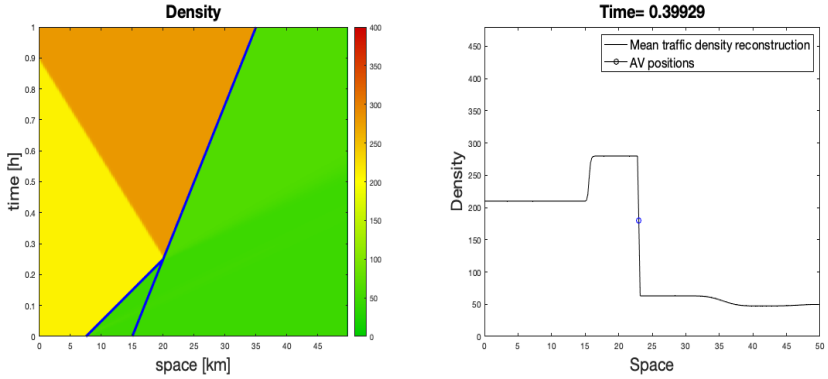

(A) Same lane interaction of an upstream active AV with an inactive one, causing the formation of a classical shock followed by a non-classical shock at the AVs' common position, see Fig. 3a.

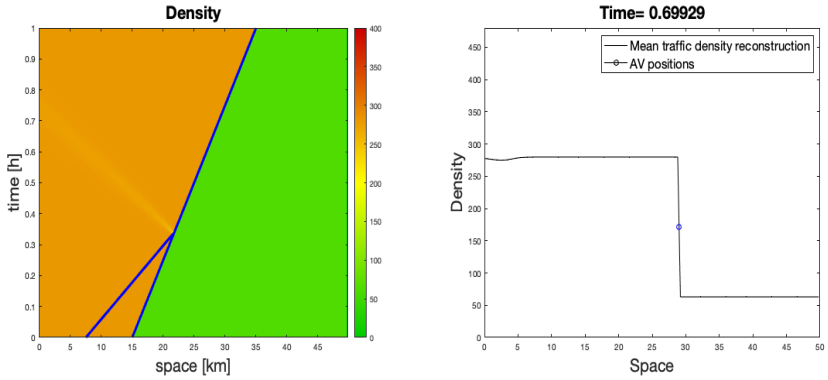

(B) Same lane interaction of an inactive AV with an active preceding one, causing no change in the surrounding traffic density displaying only a non-classical shock at the AVs' common position, see Fig. 3b.

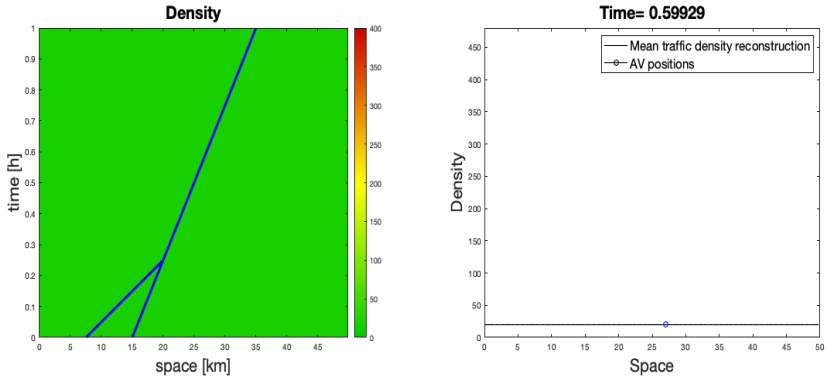

(C) Same lane interaction of inactive AVs, resulting in no change in the surrounding traffic density, see Fig. 3c.

FIGURE 5. Numerical reconstruction of possible configurations of AV interactions on same lanes. Left: (t, x) representation. Right: density profile at given time instant.

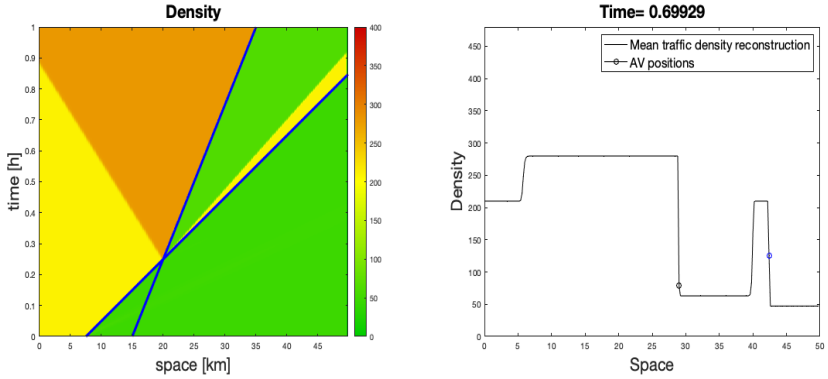

(A) Different lane interaction of an upstream active AV with an inactive one, causing the formation of two classical shocks alternated with two non-classical shocks at the AVs' positions, see Fig. 4a.

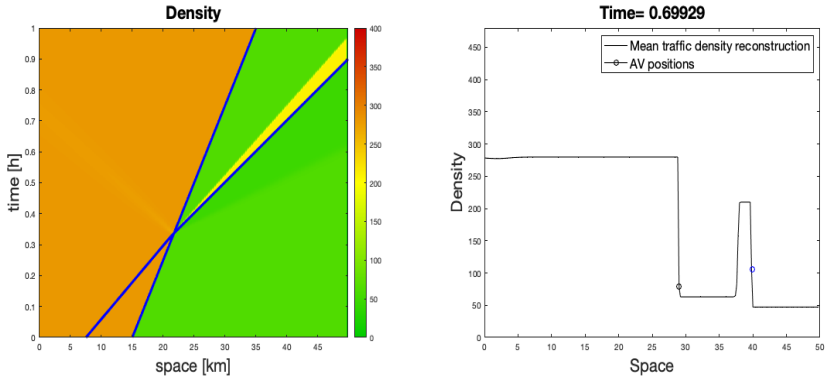

(B) Different lane interaction of an inactive AV with an active preceding one, causing the formation of a classical shock separating two non-classical shocks at the AVs' positions, see Fig. 4b.

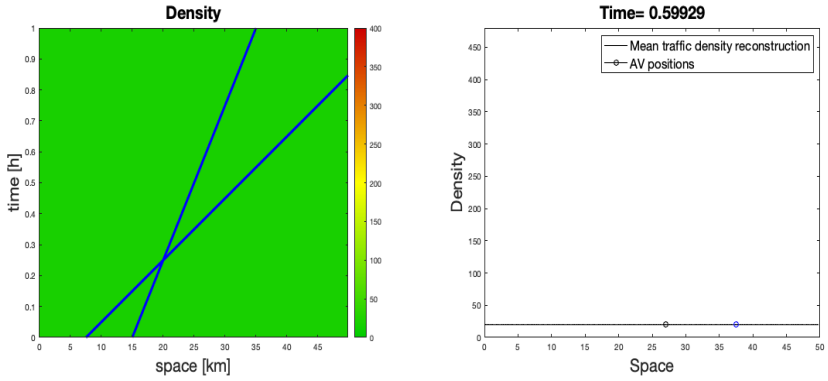

(C) Different lane interaction of inactive AVs, resulting in no change in the surrounding traffic density, see Fig. 4c.

FIGURE 6. Numerical reconstruction of possible configurations of AV interactions on different lanes. Left: (t, x) representation. Right: density profile at given time instant.

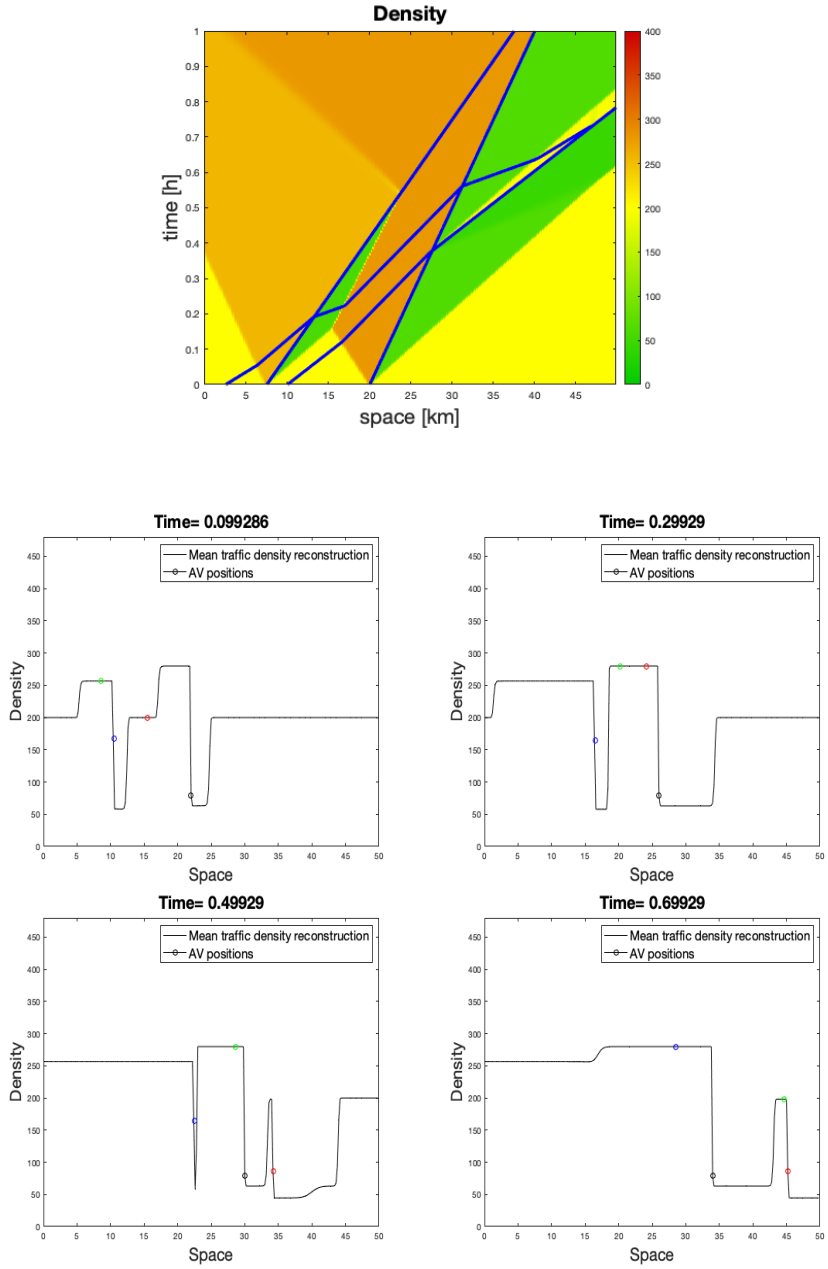

FIGURE 7. Numerical reconstruction of the solution of (1) corresponding to four interacting AVs with initial data (6). Top: (t, x) representation. Bottom: density profiles at given time instants. The first and third AV are on the same lane and merge after overtaking the others.